1982MNRAS.199..883B

Mon. Not. R. astr. Soc. (1982) **199**, 883–903

Hydromagnetic flows from accretion discs and the production of radio jets

R. D. Blandford and D. G. Payne *Theoretical Astrophysics, California Institute of Technology, Pasadena, CA 91125*

Received 1981 August 19

Summary. We examine the possibility that energy and angular momentum are removed magnetically from accretion discs, by field lines that leave the disc surface and extend to large distances. We illustrate this mechanism by solving the equations of magnetohydrodynamics, assuming infinite conductivity, for axially symmetric, self-similar, cold magnetospheric flow from a Keplerian accretion disc in which the field strength B scales with radius r as $B \propto r^{-5/4}$. We show that a centrifugally driven outflow of matter from the disc is possible, if the poloidal component of the magnetic field makes an angle of less than 60° with the disc surface. At large distances from the disc, the toroidal component of the magnetic field becomes important and collimates the outflow into a pair of anti-parallel jets moving perpendicular to the disc. Close to the disc, the flow is probably driven by gas pressure in a hot magnetically dominated corona. In this way, magnetic stresses can extract the angular momentum from a thin accretion disc and thus enable matter to be accreted, independently of the presence of viscosity. These jet solutions have the property that most of the power is concentrated within a central core, while most of the angular momentum and magnetic flux is carried near the jet walls. The relevance of this mechanism for the evolution of accretion discs around massive black holes in galactic nuclei and the production of jets in extragalactic radio sources is described.

1 Introduction

There is now direct observational evidence that extragalactic double radio sources are formed by jets emerging from the nuclei of the associated galaxies and quasars. Over 70 jets have been mapped interferometrically at radio frequences, and more than half of the double radio sources in a volume-limited sample have associated jet-like features (Bridle, private communication). These jets appear to supply the extended components with mass, energy, momentum and magnetic flux. Jets have also been detected at optical (e.g. Curtis 1918; Schmidt 1963; Butcher, van Breugel & Miley 1980) and X-ray (e.g. Feigelson *et al.* 1981) frequencies. The majority of subarcsecond radio sources bright enough to have been observed with VLBI display a one-sided core-jet morphology. In 'extended' radio sources

© Royal Astronomical Society • Provided by the NASA Astrophysics Data System

1982MNRAS.199..883B

the VLBI jets are mostly aligned with the large-scale features, suggesting that the jet collimation occurs on subarcsecond scales. In 'compact' radio sources the alignment is poorer, which is consistent with the idea that many compact sources comprise relativistic jets beamed towards us (Readhead *et al.* 1978).

Upon close examination, observed jets appear to be highly heterogeneous in their properties. Estimates of the jet velocity range from $\sim 300\,\mathrm{km\,s^{-1}}$, the escape velocity from a galaxy, to $\sim c$ for the superluminal sources (e.g. Miley 1980). Compact radio sources appear to contain very little plasma (Wardle 1977; Jones & O'Dell 1977), whereas many extended jets show evidence for depolarization (e.g. Perley, Willis & Scott 1979). Jets are associated with objects of stellar mass (e.g. Braes & Miley 1971; Margon 1982; Hjellming & Johnson 1981) as well as much larger masses in galactic nuclei. They are found in sources that appear to be accreting gas subcritically as well as supercritically. Many jets are one-sided whereas some, especially the weaker ones, are two-sided. It seems then that jet production is not a particularly specialized phenomenon, but that it can operate under widely differing conditions and indeed several distinct mechanisms may be involved.

Although there is no direct observational evidence for this, it is widely assumed that most extragalactic radio sources are formed in the vicinity of a spinning massive black hole (e.g. Lynden-Bell 1969; Zel'dovich & Novikov 1971; Rees 1978). The way in which gas flows on to a compact accreting object depends largely on the conditions where it is injected, although gas accreted by a black hole should eventually be dragged into the equatorial plane of the hole by the Lens–Thirring effect (Bardeen & Petterson 1975). The black hole and disc angular momentum axis should define the radio source axis. For gas to be swallowed by the hole it must lose its binding energy which increases inversely with the radius r. Most of the binding energy is lost in the vicinity of the inner edge of the disc and this is probably the origin of the observed nuclear luminosity, but the accreting gas must also lose its angular momentum ($\propto r^{1/2}$) mostly from the outer edge of the disc. In conventional models of accretion discs (e.g. Lynden-Bell 1969; Pringle & Rees 1972; Shakura & Sunyaev 1973), viscous or magnetic torques are invoked to transport angular momentum (and energy) outwards in the disc. In binary X-ray sources, tidal interactions with the companion star are presumably able to exert a decelerating torque on the outer parts of the disc and so the orbit provides a natural reservoir for the angular momentum liberated by the infalling matter.

However, in the case of an isolated black hole in a galactic nucleus, there is no natural sink for the orbital angular momentum. In this paper we discuss one possible resolution of this difficulty, that the angular momentum is removed magnetically by field lines that leave the disc surface, and is eventually carried off in a jet moving perpendicular to the disc.

This idea has many precedents. Most importantly, the solar wind is believed to have decelerated the Sun to its present angular momentum through the action of magnetic stresses operating over the age of the Solar System (e.g. Weber & Davis 1967; Withbroe & Noyes 1977). Similar processes may govern the contraction of proto-stellar gas clouds (e.g. Mouschovias & Paleologou 1980). Of more direct relevance are the papers of Piddington (1970), Sturrock & Barnes (1972) and Ozernoi & Usov (1973), in which twisted magnetic field lines were proposed as an explanation for double radio sources. More recently Lovelace (1976) and Blandford (1976) proposed accretion-disc models in which the energy was extracted continuously by electromagnetic torques. If, as assumed in these papers, the poloidal field lines are frozen into the spinning disc, then the electromagnetic torque per unit area, $\mathbf{T}$, does work at a rate $\mathbf{T}\cdot\boldsymbol{\omega}$, where $\boldsymbol{\omega}$ is the local Keplerian angular velocity. The ratio of the energy to the angular momentum extracted from the disc is thus ω, exactly the same ratio as that of the energy and angular momentum released when a particle in Keplerian orbit moves to a slightly smaller orbit. In these electromagnetic models, the

© Royal Astronomical Society • Provided by the NASA Astrophysics Data System

1982MNRAS.199..883B

magnetosphere above and below the disc was assumed to be force-free; that is to say, the charge density ρ_e and current density $\mathbf{J}$ satisfy $\rho_e\mathbf{E}+\mathbf{J}\times\mathbf{B}=0$. This prescription is equivalent to the neglect of inertial terms in the particle equations of motion. If jets were produced from a force-free magnetosphere like this, they would probably have relativistic expansion speeds.

It may be that the magnetosphere contains a dynamically significant density of matter. In this case a jet can still be formed and an appropriate description of its structure is possible using MHD theory, as in simple models of stellar winds. There is assumed to exist a well-defined velocity field $\mathbf{v}(\mathbf{r})$ and the perfect MHD condition, $\mathbf{E}+\mathbf{v}\times\mathbf{B}=0$, is imposed, corresponding to a high magnetic Reynold's number. This is the approach followed in the present paper. We seek self-similar magnetospheric solutions for flow from a Keplerian disc, analogous to the force-free solutions described in Blandford (1976). The field scaling in the disc is different in the MHD case and is easily derived. We anticipate that the Alfvén speed ($\propto B\rho^{-1/2}$) scales as the Keplerian velocity ($\propto r^{-1/2}$). In addition, the specific angular momentum and energy in the flow will scale as their Keplerian counterparts, which means that in a stationary flow from a stationary accretion disc, the rate of mass loss from each decade of disc radius is independent of radius. We then obtain $\rho\propto r^{-3/2}$ and $B\propto r^{-5/4}$. It is the replacement of the speed of light by the Alfvén speed that changes the scaling from that found for the electromagnetic models. If thermal effects are important, then in a self-similar flow the sound speed should also scale as $r^{-1/2}$ and so the pressure scales as $p\propto r^{-5/2}$. This has the consequence that, for a monatomic gas, the entropy does not scale with radius.

In our models, described in Sections 2 and 3, the jet is basically driven by centrifugal force and thermal effects are only of consequence close to the disc. This is in contrast to the solar wind, where the gas must be heated in the solar corona to about the escape velocity from the Sun's graviational field. Unlike the solar corona, the surface of an accretion disc is almost in free-fall and only a relatively small potential barrier need be surpassed. To see that this is so, consider purely poloidal magnetic field lines emerging from the surface of an accretion disc (*cf.* Fig. 1), along which cold gas can flow. The magnetic field lines are frozen into and convected by the disc (Ferraro's 1937 law of isorotation), while the elements of relatively tenuous gas on the field lines behave like beads on a rigid wire (*cf.* Henriksen & Rayburn 1971). If the 'beads' start from rest at the disc and are carried with constant angular velocity by the 'wire', then the equipotential surfaces can be calculated (Fig. 1). From these we see that, provided the poloidal component of the magnetic field makes an angle of less than 60° to the outward radius vector at the disc surface, then gas will be flung outwards. Of course, thermal effects can alter this condition somewhat, but this mechanical analogy does exhibit the essential dynamical feature of a centrifugally driven outflow.

Again, as in the solar wind, inertial stresses are probably small compared with magnetic stresses close to the start of the flow, and the field lines will be largely force-free and therefore bent towards the rotation axis because of the balance of the magnetic pressure gradient by magnetic tension. At large distances from the disc, the inertia of the gas will cause the magnetic field to become increasingly toroidal. This introduces a magnetic 'hoop' stress which causes further collimation. Thus the magnetic stresses operating in these two ways are responsible for the conversion of a centrifugal outflow into a collimated jet.

We have confined our attention to self-similar solutions (Section 2) because they provide the simplest means of showing that the mechanism just outlined qualitatively can indeed operate in a self-consistent manner. A realistic accretion disc must be far more complicated. Magnetic stresses operating within the disc can undoubtedly transfer angular momentum from one radius to another and magnetic instability can lead to reconnection and quite complex field geometry. It is entirely possible that, again as is true of the Sun, the open field

© Royal Astronomical Society • Provided by the NASA Astrophysics Data System

1982MNRAS.199..883B

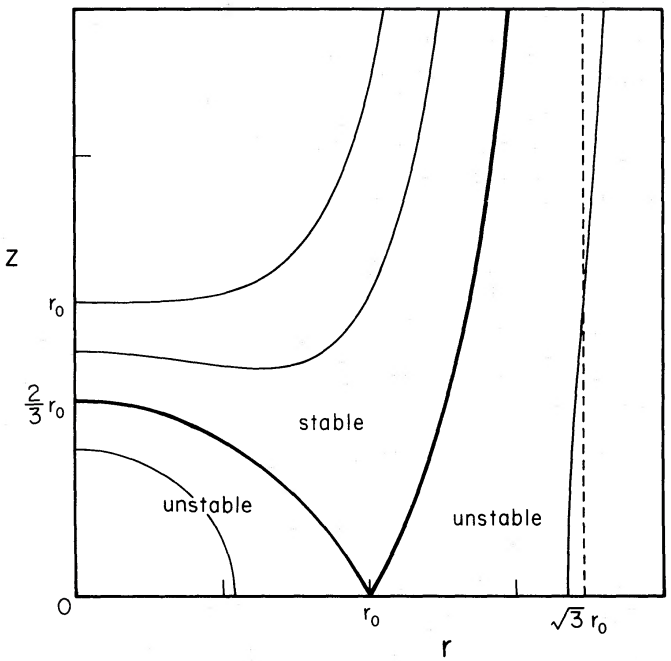

Figure 1. Equipotential surfaces for a bead on a wire, corotating with the Keplerian angular velocity $(GM/r_0^3)^{1/2}$ at a radius r_0, which is released from rest at r_0. The equation of the surfaces is

$$\phi(r,z) = -\frac{GM}{r_0}\left[\tfrac{1}{2}\left(\frac{r}{r_0}\right)^2 + \frac{r_0}{(r^2+z^2)^{1/2}}\right] = \text{constant}.$$

The surfaces are separated by equal intervals in $\phi(r,z)$. If the projection of the wire on the meridional plane makes an angle of less than 60° with the equatorial plane, the equilibrium at $r=r_0$ is unstable. If the angle is greater than 60°, the equilibrium is stable. The dashed line at $r=\sqrt{3}r_0$ is the asymptote for the surface of marginal stability which reaches infinity in the z-direction.

lines may emerge from only a relatively small fraction of the disc surface. For this reason, the numerical results quoted in Section 3 are only intended to be illustrative. At large distances from the disc where we propose a jet will have formed, the self-similarity hypothesis – all quantities scale as power-laws of *spherical* radius along a given direction – becomes increasingly artificial. It is far more natural to describe the jet structure by solutions that are self-similar in *cylindrical* radius as has been done by Chan & Henriksen (1980) and Bicknell & Henriksen (1980).

As most of the energy and angular momentum of the gas in the disc is extracted by magnetic torques, the fraction of the accreted gas that must flow in the jet can be quite small. This, in turn, implies that the scale height of the disc corona can be small compared with the radius. Hence we can simplify the problem by regarding the gas as being cold and starting from rest at the equatorial plane, as we do in Section 2. In fact, the gas must be driven by thermal pressure away from a disc corona through a critical point and become supersonic, but strongly sub-Alfvénic, before it has moved very far from the disc. This part of the flow is analysed in Section 4.

A discussion of the general features of this model and its observational ramifications is given in Section 5.

2 Self-similar MHD solution

2.1 MHD EQUATIONS

The equations of stationary, axisymmetric MHD flow in cylindrical co-ordinates (r, ϕ, z)

© Royal Astronomical Society • Provided by the NASA Astrophysics Data System

1982MNRAS.199..883B

have been written down by several authors (e.g. Chandrasekhar 1956; Mestel 1961). The fluid velocity $\mathbf{v}(\mathbf{r})$ is related to the field strength $\mathbf{B}(\mathbf{r})$ by

$$\mathbf{v} = \frac{k\mathbf{B}}{4\pi\rho} + (\boldsymbol{\omega} \times \mathbf{r}), \tag{2.1}$$

where the undetermined constant $k/4\pi$ (which can be interpreted as the ratio of the constant mass flux to the constant magnetic flux) and the angular velocity ω satisfy

$$(\mathbf{B} \cdot \nabla)\, k = (\mathbf{B} \cdot \nabla)\, \omega = 0.$$

There are two constants of the motion, the specific energy

$$e = \tfrac{1}{2}v^2 + h + \Phi - \frac{\omega r B_\phi}{k}, \tag{2.2}$$

and the specific angular momentum

$$l = r v_\phi - \frac{r B_\phi}{k}; \tag{2.3}$$

that is,

$$(\mathbf{B} \cdot \nabla)\, e = (\mathbf{B} \cdot \nabla)\, l = 0.$$

In equation (2.2), h is the enthalpy per unit mass, Φ is the gravitational potential and the term $-\omega r B_\phi/k$ represents the work done on the streaming gas by the magnetic torque, given by the second term in equation (2.3).

The gas density is obtained from the continuity equation,

$$\nabla \cdot (\rho \mathbf{v}) = 0. \tag{2.4}$$

Finally, we need the z-component of the momentum equation

$$\rho (\mathbf{v} \cdot \nabla)\, v_z = -\frac{\partial p}{\partial z} - \frac{\rho \partial \Phi}{\partial z} - \frac{1}{8\pi}\frac{\partial B^2}{\partial z} + \frac{1}{4\pi}(\mathbf{B} \cdot \nabla) B_z, \tag{2.5}$$

p being the gas pressure, to specify the problem fully.

2.2 SELF-SIMILAR SOLUTIONS

As described in the introduction, we seek a self-similar solution for axisymmetric flow from an accretion disc in Keplerian orbit about a black hole of mass M, with $B(r, \phi, 0) \propto r^{-5/4}$. For the field lines meeting the disc at radius r_0, we introduce the scaling

$$\mathbf{r} = [r_0 \xi(\chi), \quad \phi, \quad r_0 \chi] \tag{2.6a}$$

$$\mathbf{v} = [\xi'(\chi) f(\chi), \quad g(\chi), \quad f(\chi)] \left(\frac{GM}{r_0}\right)^{1/2}, \tag{2.6b}$$

so that all quantities will scale with spherical radius along a given direction. In equations (2.6) a subscript '0' indicates a quantity evaluated at the disc surface ($\chi = 0$ and $\xi = 1$) and a

© Royal Astronomical Society • Provided by the NASA Astrophysics Data System

1982MNRAS.199..883B

prime denotes differentiation with respect to χ. We also introduce the dimensionless parameters

$$\epsilon \equiv \frac{e}{(GM/r_0)} \tag{2.7a}$$

$$\lambda \equiv \frac{l}{(GMr_0)^{1/2}} \tag{2.7b}$$

$$\kappa \equiv k\,(1+\xi_0'^2)^{1/2}\,\frac{(GM/r_0)^{1/2}}{B_0}, \tag{2.7c}$$

with B_0 the poloidal field strength at the disc surface; ϵ, λ, κ and ξ_0' are constant parameters that define the solution. If the flow is adiabatic with specific heat ratio γ, an extra parameter μ enters the problem,

$$\mu \equiv \frac{p}{(B_0^2/4\pi)}\left(\frac{B_0^2 r_0}{4\pi\rho GM}\right)^{\gamma}. \tag{2.7d}$$

We then find that the density is related to the field geometry through the continuity condition

$$\rho\xi f J = (\rho f)_0, \tag{2.8}$$

where

$$J = \xi - \chi\xi'. \tag{2.9}$$

2.3 COLD MHD FLOW

If the flow becomes supersonic very close to the disc, where it is still highly sub-Alfvénic, we can ignore the thermal terms in equations (2.2) and (2.5) and treat the flow as starting with the Keplerian velocity at the disc, i.e. $\omega = (GM/r_0^3)^{1/2}$, $g_0 = 1$, $f_0 = 0$. Combining the energy and angular momentum equations we obtain,

$$\begin{aligned}\epsilon - \lambda &= \tfrac{1}{2}\,[f^2 U + g^2 - 2g\xi] - S \\ &= -3/2,\end{aligned} \tag{2.10}$$

where

$$U = (1+\xi'^2) \tag{2.11a}$$

$$S = (\xi^2+\chi^2)^{-1/2}. \tag{2.11b}$$

We next substitute for g from the ϕ-component of equation (2.1). This yields a quartic for $f(\chi)$,

$$T - f^2 U = \left[\frac{(\lambda-\xi^2)\,m}{\xi(1-m)}\right]^2 \tag{2.12}$$

© Royal Astronomical Society • Provided by the NASA Astrophysics Data System

1982MNRAS.199..883B

where

$$m \equiv \frac{4\pi\rho\,(v_r^2 + v_z^2)}{(B_r^2 + B_z^2)} \tag{2.13a}$$

$$= \kappa\xi\, fJ \tag{2.13b}$$

and

$$T = \xi^2 + 2S - 3. \tag{2.14}$$

m can be interpreted as the square of the Alfvén Mach number. $-\frac{1}{2}T(\xi, \chi)$ is the gravitational plus centrifugal potential difference between the point (ξ, χ) and the disc $(1, 0)$. For a physical solution $T \geqslant 0$ (*cf.* Fig. 1). We wish to solve the equations for the structure of the field lines, and hence for the flow variables as a function of χ. This is done by combining the z-component of the momentum equation, equation (2.5),

$$\alpha m' + \beta\xi'' + \gamma = 0, \tag{2.15a}$$

where

$$\alpha = \xi\,(mf^2 J - \xi T) \tag{2.15b}$$

$$\beta = \chi m\,(m-1)\,\xi f^2 \tag{2.15c}$$

$$\gamma = m\,[5/4\,\xi T\xi' - (m-1)\,f^2 J\xi' + \chi m\xi J S^3 + (1 - S^3)\,\xi^3\xi' - \chi\xi^2 S^3], \tag{2.15d}$$

with the differential form of the quartic for $f(\chi)$, equation (2.12),

$$\delta m' + \epsilon\xi'' + \theta = 0, \tag{2.16a}$$

where

$$\delta = (m-1)\,(mf^2 U - T)\,\xi J \tag{2.16b}$$

$$\epsilon = m\,(m-1)^2(\chi + \xi\xi')\,\xi f^2 \tag{2.16c}$$

$$\theta = 2m^3(\xi^2 - \lambda)\,J\xi' - m\,(m-1)^2 J\,[T\xi' + (1 - S^3)\,\xi^2\xi' - \chi\xi S^3], \tag{2.16d}$$

to obtain a second-order differential equation for $\xi(\chi)$,

$$\begin{aligned}\xi f^2 T(m-1)^2(t-1)\,\xi'' + JS^2\,\{&(m-1)^2\,[\xi T + (n-m-1)f^2 J]\,T \\ &+ m\,(m-1)\,[(t-1)\,\xi TS - \xi f^2(\chi + \xi\xi')\,(\xi\xi' - \xi\xi' S^3 - \chi S^3)] \\ &+ (m-1)\,[m\xi^2(\xi T - mf^2 J) - 5/4\,(n-1)\,\xi T^2] + 2m^2(\xi^2 - \lambda)\,(mf^2 J - \xi T)\} = 0\end{aligned} \tag{2.17}$$

where

$$t \equiv \frac{4\pi\rho v_\theta^2}{B^2} \tag{2.18a}$$

$$= \kappa\xi f^3 J^3 S^2/T, \tag{2.18b}$$

$$n \equiv \frac{4\pi\rho\,(v_r^2 + v_z^2)}{B^2} \tag{2.19a}$$

$$= \kappa\xi f^3 JU/T. \tag{2.19b}$$

n is the square of the Mach number for the fast magnetosonic mode. t has a more subtle interpretation and is discussed below. In equation (2.18a), v_θ is the fluid velocity in the θ-direction in spherical geometry. Equations (2.12) and (2.17) fully specify the flow and a

© Royal Astronomical Society • Provided by the NASA Astrophysics Data System

1982MNRAS.199..883B

solution can be obtained by integrating equation (2.17) numerically using the initial conditions $\xi(0)=1$ and $\xi'(0)=\xi'_0$, with f given implicitly by equation (2.12).

2.4 CRITICAL POINTS

Critical points of the differential equation usually arise in stationary flows where the fluid velocity equals the speed of a backward-propagating disturbance. As such, they are a relic of the initial conditions, since the waves are propagating along the characteristics of the time-dependent equations. There are two appropriate waves in this problem, the non-compressive Alfvén mode and the compressive fast magnetosonic mode. The mathematical behaviour of the solutions is most transparent if we replace equation (2.17) with the equation for the Alfvén Mach number,

$$m'=\frac{mS^2\{2m^2\chi(\xi^2-\lambda)J-(m-1)(5/4T+\xi^2-S)\xi(\chi+\xi\xi')-(m-1)^2[\chi(\xi^2+T)-f^2(\chi+\xi\xi')]J\}}{\xi T(m-1)(t-1)}. \tag{2.20}$$

This equation has two important possible singularities. Firstly, when $m=1$, the denominator becomes zero and so, for a physical solution to pass through $m=1$, the numerator must also be zero. This implies that $\xi=\lambda^{1/2}$, the usual condition for an Alfvén critical point (*cf.* Weber & Davis 1967). However, in this problem the interpretation is somewhat more subtle than in spherically symmetric problems. Our flow has, by mathematical assumption, been constrained to be both axisymmetric and self-similar. This is also true of the corresponding time-dependent problem and so the only waves that can propagate have their **k**-vectors perpendicular to the surfaces of self-similarity. Our original similarity hypothesis, equations (2.6), ensures that all flow variables scale as prescribed power-laws with spherical radius R along a spherical radius direction. So the waves propagate along the $\hat{\boldsymbol{\theta}}$ direction (where θ is the usual spherical polar angle). The critical condition is then that the wave speed along $\hat{\boldsymbol{\theta}}$ equals $(\mathbf{v}\cdot\hat{\boldsymbol{\theta}})$. For the Alfvén mode, which propagates with a phase speed $(\hat{\mathbf{k}}\cdot\mathbf{B})/(4\pi\rho)^{1/2}$, this condition becomes $m=1$. Likewise, for the fast mode, which propagates with a phase speed $|\mathbf{B}|/(4\pi\rho)^{1/2}$, the critical condition can be shown to correspond to the second singularity of equation (2.20), $t=1$.

Now we are interested in solutions in which the flow becomes increasingly collimated parallel to the z-axis and in which the field becomes increasingly toroidal. As will be clear from Section 2.6, this implies that $t<1$ even at large distances from the disc, despite the fact that both m and n (the square of the fast-mode Mach number) become much larger than unity. Therefore our solutions for the cold flow pass through only one critical point, where $m=1$. An analogous result is true for the gas-dynamical self-similar solutions of Bardeen & Berger (1978). (When thermal terms are included, there is an additional critical point associated with the slow magnetosonic wave, *cf.* Section 4 below.)

From equations (2.12) and (2.20) it can be shown, using L'Hôpital's rule, that

$$m'=\frac{2\xi'}{(T-f^2U)^{1/2}} \tag{2.21}$$

at the Alfvén critical point. This relation can be used as a means for integrating across the critical point.

Although there is no critical point in our self-similar solutions when the fast-mode Mach

© Royal Astronomical Society • Provided by the NASA Astrophysics Data System

1982MNRAS.199..883B

number is unity (i.e. $n=1$), this point still manifests itself in equation (2.12). When $n=1$ the quartic in f, equation (2.12), reduces to

$$T=\frac{(\xi^2-\lambda)^2 m^3}{\xi^2(m-1)^3}, \tag{2.22}$$

corresponding to a confluence of two of the roots. This can be interpreted as the point where our outgoing solution intersects the corresponding incoming solution, as typically occurs at a critical point. However, it can be shown that our outgoing solutions will pass smoothly through this point to yield solutions in which the fast-mode Mach number exceeds unity, without any additional constraint having to be satisfied. (The incoming solutions have the inverse property.)

2.5 SOLUTION CLOSE TO THE DISC

The presence of large-scale magnetic fields dominating the region above the disc makes it dynamically feasible for centrifugal forces to drive gas from the disc along the field lines, as discussed in Section 1. Magnetic stresses rapidly become important though, and the magnetic pressure plays a significant role in accelerating the gas out to the point where the bulk velocity exceeds the fast-mode wave speed (and long after the centrifugal forces have ceased being important).

Close to the disc we can expand equations (2.12) and (2.17) about $\chi=0$ and $\xi=1$ to obtain the appropriate solutions for the fluid velocity and the shape of the field lines. We find

$$f=f_0'\chi+\tfrac{1}{2}f_0''\chi^2+\ldots, \tag{2.23a}$$

$$\xi=1+\xi_0'\chi+\tfrac{1}{2}\xi_0''\chi^2+\ldots, \tag{2.23b}$$

where

$$f_0'=\frac{(3\xi_0'^2-1)^{1/2}}{[\kappa^2(\lambda-1)^2+(1+\xi_0'^2)]^{1/2}}, \tag{2.23c}$$

$$f_0''=\frac{-9\kappa\xi_0'^2-\tfrac{1}{4}\left[3\kappa^2(\lambda-9)(\lambda-1)+5(1+\xi_0'^2)\right]\xi_0' f_0'+\kappa(2+3\xi_0'^2)f_0'^2+2\xi_0' f_0'^3+2\kappa f_0'^4}{(3\xi_0'^2-1)}, \tag{2.23d}$$

$$\xi_0''=-1-\tfrac{1}{4}(1+\xi_0'^2)+\kappa(1-3/f_0'^2)\xi_0' f_0'-\tfrac{1}{4}\kappa^2(\lambda-9)(\lambda-1). \tag{2.23e}$$

These solutions can be used to begin the numerical integrations. Equations (2.23c) and (2.23d) demonstrate the point made in Section 1 that an angle of 60° between the disc and the poloidal magnetic field is the critical one for initiating a flow.

2.6 FAR-FIELD SOLUTION

At large distances above the disc, the field is predominantly toroidal. The tension in the field provides the means for collimating the flow in the far-field. The shape of the field lines will then be determined by a balance between the inwardly directed hoop stress and the outwardly directed magnetic pressure. Although the flow is centrifugally driven, centrifugal

© Royal Astronomical Society • Provided by the NASA Astrophysics Data System

1982MNRAS.199..883B

forces are unimportant far from the disc. To see this, we note that the ratio of the centrifugal force to the force associated with the magnetic tension is

$$\frac{4\pi\rho v_\phi^2}{B_\phi^2} = \frac{(m\lambda - \xi^2)^2}{m(\xi^2 - \lambda)^2}. \tag{2.24}$$

At large distances from the disc, $m = 0(\xi^2)$ and hence for $\lambda \gtrsim 0(1)$ the ratio (2.24) is $0(\xi^{-2})$, so the centrifugal force cannot support the jet against constriction by the magnetic tension.

To obtain approximate solutions to the far-field flow we expand equations (2.2) and (2.17) in powers of ξ^{-2} assuming that $\xi^2/\chi^2 \ll 1$ and $\xi' \ll 1$. The asymptotic form of the energy equation is

$$(\lambda - 3/2) = \tfrac{1}{2}f^2 + \frac{\xi}{\kappa f J}; \tag{2.25}$$

while the asymptotic form of equation (2.17) can be simplified to

$$\xi\chi^2\xi'' + J\chi\xi' + \tfrac{1}{4}\xi J - \frac{1}{4\kappa f^3}\xi^2 = 0. \tag{2.26}$$

These equations admit two types of super-Alfvénic flow.

(i) *The solution asymptotically approaches* n = 1 *as* $\chi \to \infty$
We find

$$f_\infty = \left(\frac{2\lambda - 3}{3}\right)^{1/2}, \tag{2.27}$$

$$\xi = c_1 \chi^{\alpha_1}, \tag{2.28}$$

$$m = \frac{3c_1^2}{(2\lambda - 3)}\chi^{2\alpha_1}, \tag{2.29}$$

with

$$\alpha_1 = 1 - 3^{3/2}/\beta, \tag{2.30}$$

$$\beta \equiv \kappa(2\lambda - 3)^{3/2} \gg 1. \tag{2.31}$$

The constant c_1 must be found by numerical integration of the full equations from $\chi = 0$, $\xi = 1$. Also, for a given value of κ, λ is an eigenvalue of the flow such that $n \to 1$ as $\chi \to \infty$. Flows with this asymptotic behaviour have $\xi'_\infty \to 0$ and hence are parallel to the z-axis far from the disc. From equations (2.25) and (2.27) we see that one-third of the available energy is carried off in the form of bulk kinetic energy associated with the poloidal flow, while two-thirds of the available energy is transported out by the magnetic field and can be associated with the Poynting flux.

(ii) *The solution attains* n > 1 *at finite height above the disc*
We find here

$$f_\infty = (2\lambda - 3)^{1/2}\left(1 - \frac{1}{\beta c_2 \chi^{1/4}}\right) \tag{2.32}$$

$$\xi = c_1 \chi^{\alpha_2} \exp(-4c_2\chi^{1/4}), \tag{2.33}$$

$$m = \frac{c_1^2 c_2 \beta}{(2\lambda - 3)}\chi^{1/4 + 2\alpha_2}\exp(-8c_2\chi^{1/4}), \tag{2.34}$$

$$n = \beta c_2 \chi^{1/4}\left(1 - \frac{2}{\beta c_2 \chi^{1/4}}\right) \gg 1, \tag{2.35}$$

© Royal Astronomical Society • Provided by the NASA Astrophysics Data System

1982MNRAS.199..883B

with

$$\alpha_2 = 1 - 1/\beta. \tag{2.36}$$

The constants c_1 and c_2 must be found by numerical integration of the full equations from $\chi = 0$, $\xi = 1$. These solutions correspond to flows in which n becomes arbitrarily large. Note, however, that there is a 'turning-point' in the radial excursion of the field line. This turning point occurs when n attains the critical value

$$n_t \equiv \beta - 3. \tag{2.37}$$

With $n < n_t$, gas is accelerated along the field lines to larger radii as well as greater height above the disc. When $n > n_t$ though, the radial velocity becomes negative and the flow converges towards the z-axis as it is accelerated to greater and greater heights above the disc. This type of behaviour can be understood by considering the asymptotic form of the energy equation, equation (2.25). The first term on the right-hand side of this equation represents the bulk kinetic energy associated with the poloidal motion, while the second term represents the magnetic energy. For cold MHD, the requirement that the fast magnetosonic Mach number exceed unity is essentially the requirement that the kinetic energy flux dominates the Poynting flux. But the work done by the magnetic field will always be a significant contribution to the total energy unless the field lines approach the z-axis. This is because with our cold MHD flows, the jet is supported in the transverse direction by the magnetic field. As a consequence, in flows which have the asymptotic behaviour $\xi'_\infty \to 0$ and in which the cross-sectional area of the jet continues to increase, the work done by the magnetic field must be significant even at infinity and hence correspond to $n = 1$ far from the disc. Flows with $n > 1$ need not be completely choked-off though, since, at small radii, centrifugal forces will again become important. Also, when thermal effects are included, the jet can be supported in the transverse direction by gas pressure. The magnetic contribution to the total energy can become arbitrarily small as long as the gas pressure gradient is sufficient to support the jet against the magnetic tension. Dissipation in the converging flow may heat the gas enough to provide this pressure.

The choking-off of the flow in our models with $n > 1$ need not be a worry then, and arises only because of our neglect of gas pressure. By analogy with our $n = 1$ flows, we anticipate that such flows can exist with well-behaved asymptotic behaviour.

There also exist flows with $n < 1$ at infinity, having characteristically low velocities and little collimation. As a result we do not consider them here.

3 Numerical results

We have integrated equation (2.17) numerically for different values of the three independently adjustable parameters ξ'_0, κ and λ. We are interested in solutions that become super-Alfvénic ($m > 1$) at a finite height above the disc. The solutions must then pass through a critical point. We find that, for suitable choices of κ and λ, there is a value of ξ'_0 such that the solution passes through the critical point $m = 1$, $\xi = \lambda^{1/2}$ and then becomes super-Alfvénic. In this way we have been able to determine the character of the solutions as a function of the angular momentum parameter λ and the parameter κ describing the ratio of particle to magnetic flux. These results are shown in Fig. 2. $\mathrm{Cotan}^{-1}(\xi'_0)$ is the angle the poloidal field makes with the disc as it leaves the surface of the disc. We have plotted the contours of constant ξ'_0 in the (κ, λ)-plane. In Section 2.6 we found that the solutions in the far-field depended on κ and λ through the quantity $\beta = \kappa(2\lambda - 3)^{3/2}$. We have also plotted various values of β in Fig. 2. The solutions are sensitive to β in such a way that, for large β, gas is

© Royal Astronomical Society • Provided by the NASA Astrophysics Data System

1982MNRAS.199..883B

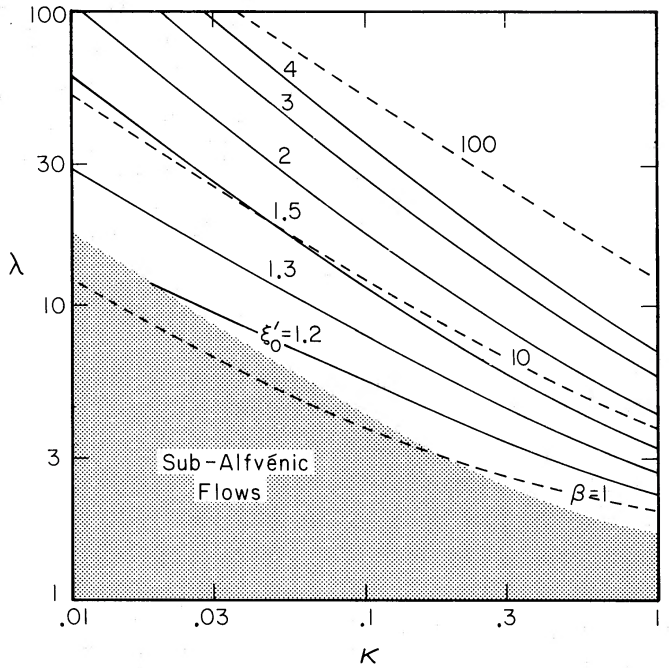

Figure 2. Possible flows as a function of κ and λ. For $\kappa\lambda(2\lambda-3)^{1/2}<1$, the flow will always remain sub-Alfvénic ($4\pi\rho v_p^2<B_p^2$); while, for $\kappa\gtrsim 1$, the flow is particle-dominated and has relatively little collimation. Only in the unhatched region are super-Alfvénic ($4\pi\rho v_p^2>B_p^2$), magnetically collimated flows possible. The requirement that the solution pass through the critical point $4\pi\rho v_p^2=B_p^2$, $\xi^2=\lambda$ fixes ξ_0'. Various values of ξ_0' are represented by the solid lines. The parameter $\beta=\kappa(2\lambda-3)^{3/2}$ which controls the asymptotic behaviour of the solutions is also plotted.

driven, by centrifugal force, to a large radius before the magnetic field is able to collimate the flow. For small β the converse is true.

Not all values of κ and λ are capable of producing super-Alfvénic flows at infinity. A minimum value of λ, $\lambda_{\min}$, which enables the flow to reach the Alfvén point at a finite height above the disc satisfies

$$\kappa\lambda_{\min}(2\lambda_{\min}-3)^{1/2}=1. \tag{3.1}$$

In general the value of λ which allows the flow to be super-Alfvénic at infinity is larger than this value. (Note that the requirement $\lambda>\lambda_{\min}$ is roughly equivalent to the constraint $\beta>1$.) We have restricted ourselves to solutions with $\kappa<1$ in order that the flow be magnetically dominated in the vicinity of the disc. For illustrative purposes we isolate one 'standard' solution (corresponding to $\kappa=0.03$, $\lambda=30$ and $\xi_0'=1.58$). In Fig. 3 we have plotted the streamlines projected into the poloidal plane for this standard case. The dashed line illustrates the self-similar scaling; each field line intersects the dashed line with the same angle, and corresponds to the location of the $m=1$ surface. Also plotted is the pitch angle of the field $\alpha(\equiv\tan^{-1}|B_\phi/B_p|)$, illustrating the way in which the inertia of the gas causes the magnetic field to become increasingly toroidal. The Alfvén Mach number, measured along the field line, is displayed in Fig. 4, together with the fast magnetosonic Mach number, the poloidal velocity, the toroidal velocity and the ratio of the toroidal field strength to the poloidal field strength. θ is the polar angle as measured from the origin of the coordinate system. We have also indicated the location of the Alfvén critical point and the point where the fast-mode Mach number is unity. Note that the azimuthal velocity increases until the Alfvén critical point is almost reached as the matter accelerated along the field line by the

© Royal Astronomical Society • Provided by the NASA Astrophysics Data System

1982MNRAS.199..883B

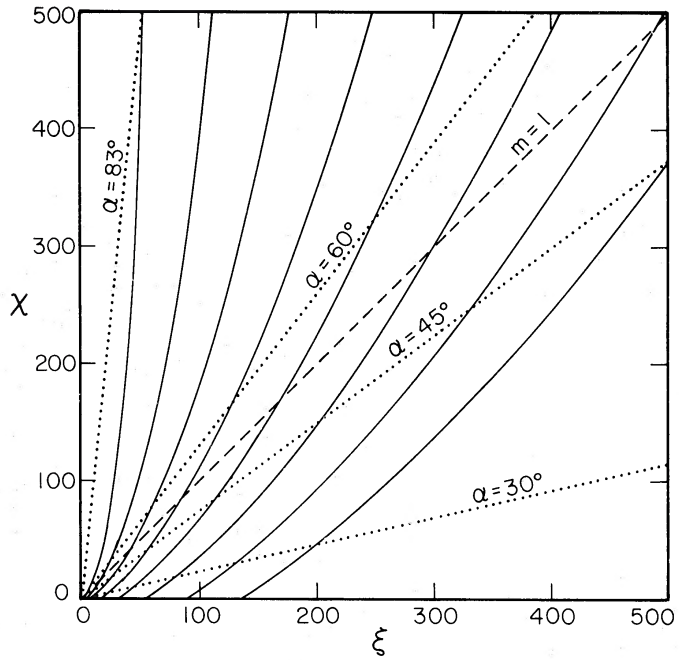

Figure 3. Flow streamlines projected into the poloidal plane for the 'standard' solution $\kappa = 0.03$, $\lambda = 30$. The dashed line illustrates the self-similar scaling, each field line intersects the dashed line with the same angle, and corresponds to the location of the $m = 1$ surface. Due to the self-similarity, the figure will be unchanged if the r and z axes are scaled by the same factor. For this case, $\xi'_\infty = 0.03$, corresponding to a jet opening angle of $\theta = 6°$. Also plotted is the pitch angle $\alpha = \tan^{-1} |B_\phi / B_p|$ of the magnetic field, illustrating the way in which the inertia of the matter causes the field to become increasingly toroidal.

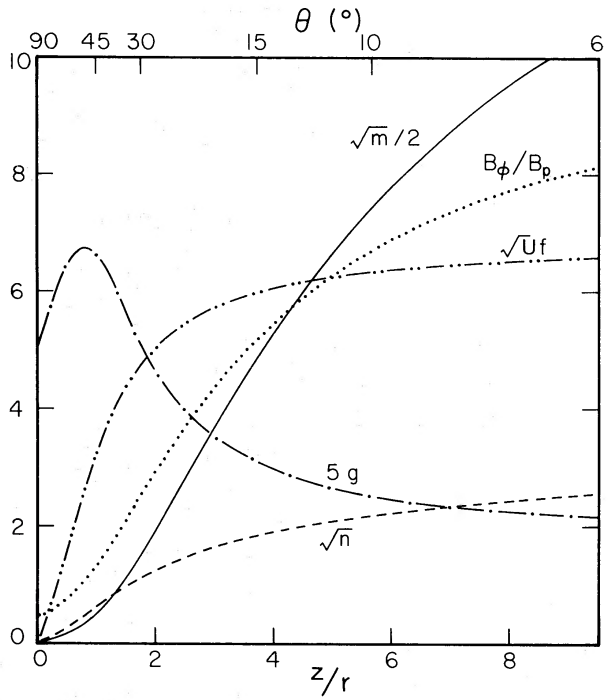

Figure 4. The Alfvén Mach number $m^{1/2}$, the fast magnetosonic Mach number $n^{1/2}$, the poloidal velocity $U^{1/2}f$, the toroidal velocity g, and the ratio of the toroidal field strength to the poloidal field strength along a single streamline.

© Royal Astronomical Society • Provided by the NASA Astrophysics Data System

1982MNRAS.199..883B

Table 1. Characteristic parameters of the standard solution – radial displacement of the streamline ξ, cotangent vector to the streamline ξ', poloidal velocity $U^{1/2}f$, azimuthal velocity g (all in dimensionless units, see Section 2.2), Alfvén Mach number $m^{1/2}$, fast magnetosonic Mach number $n^{1/2}$ and the component of the fast magnetosonic Mach number resolved perpendicular to the surfaces of self-similarity $t^{1/2}$ (see Section 2.4) – evaluated at various heights above the disc – the surface of the disc, the Alfvén critical point, the point where the fast magnetosonic Mach number is unity, after the flow has risen two decades in height above the disc, and at $\chi_{max} = 500$, where we terminated the solution.

$\kappa = 0.03, \lambda = 30$

χ	ξ	ξ'	$U^{1/2}f$	g	$m^{1/2}$	$n^{1/2}$	$t^{1/2}$
0	1	1.58	0	1	0	0	0
5.46	5.48	0.60	3.17	1.33	1	0.61	0.15
16.3	10.6	0.39	4.40	1.10	2.34	1	0.19
100	28.8	0.14	5.74	0.65	8.64	1.73	0.23
500	53.8	0.03	6.59	0.43	20.7	2.55	0.20

magnetic stresses. Beyond this point the inertia of the matter dominates the azimuthal flow and the azimuthal velocity decreases as the matter attempts to conserve its angular momentum independently of the magnetic field. However, in this solution, the flow never quite reaches a point where this is strictly true, and hence, even at great distances from the disc, there is still a small current in the z-direction. The poloidal velocity increases until approximately the point where the fast-mode Mach number is unity. This is beyond the point where the centrifugal force is important and demonstrates how the matter is also accelerated by the magnetic pressure gradient.

As discussed in Section 1, the self-similar scaling with spherical radius becomes artificial very far from the disc, so we have chosen to stop the solutions at some arbitrary height above the disc. For our standard model, this was after somewhat more than two and a half decades of radius and height. As our primary purpose in these calculations has only been to demonstrate the existence of these solutions and not to produce a serious model of a jet, we see no problem with an arbitrary termination of the solution. Table 1 displays the characteristics of the standard solution at the surface of the disc, the Alfvén critical point, the point where the fast magnetosonic Mach number is unity, after the jet has gone two decades in height above the disc, and $\chi_{max} = 500$, where we terminated the solution. For this case, $\xi'_\infty = 0.03$, corresponding to a jet opening angle of 6° when the solution was terminated.

4 Thermal effects

As described in Section 1, it is not strictly consistent to regard the flow as starting from rest from an infinitely thin disc where the radial component of magnetic field is discontinuous. A more likely geometry is illustrated in Fig. 5. For a disc of finite but small thickness we expect that the field lines would pass through a 'corona' within which they would bend from near vertical to make an angle $\sim \cot^{-1}\xi'_0$ with the disc. When $\xi'_0 \gtrsim 1/\sqrt{3}$, particles will be flung outwards under centrifugal force from the 'corona'. These must be re-supplied by gas driven upwards by the pressure in the disc.

If the surface of the Sun is any guide, the field geometry and coronal structure are likely to be highly complex. In particular, the corona will be inhomogeneous and non-steady. It is probably reasonable to expect that open field lines emerge from only a fairly small fraction of the disc and that these are held in equilibrium by the magnetic stresses associated with the closed field loops. Provided that the plasma has low $\beta (\equiv p_{gas}/p_{magnetic})$, there is no necessity to impose a horizontal force balance as we have done in the outer parts of the magneto-

© Royal Astronomical Society • Provided by the NASA Astrophysics Data System

1982MNRAS.199..883B

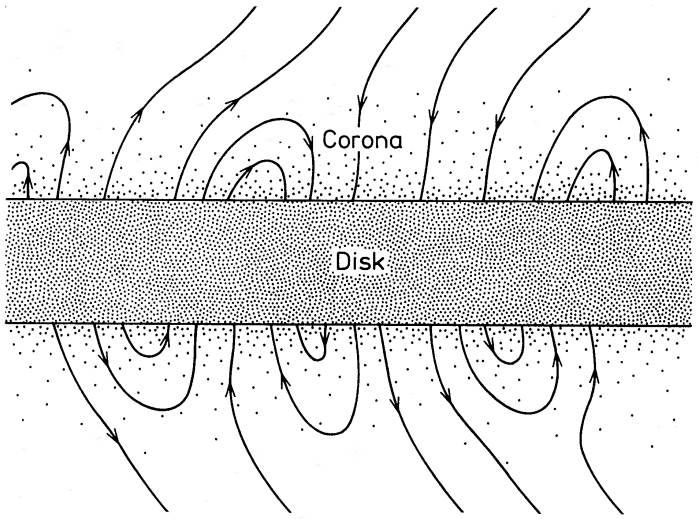

Figure 5. A schematic representation of a possible field geometry close to the disc.

sphere. As the flow is believed to be established within a few pressure scale heights of the disc, the outflow velocity will be roughly sonic, but by assumption, quite sub-Alfvénic. There will then be a sonic point in the flow associated with the slow magnetosonic wave.

As a simple illustration of the type of flow under consideration, consider field lines that have a particular profile close to the disc. Assume further that the flow is maintained isothermal with a sound speed s. We can then introduce coordinates x, y scaled to the pressure scale height $\sim s/\omega \ll r_0$,

$$x = \omega r_0 (\xi - 1)/s \tag{4.1}$$

$$y = \omega r_0 \chi/s, \tag{4.2}$$

where ω is the Keplerian angular velocity at r_0. Let the field line lie in a plane making an angle ζ with the meridional plane such that

$$\tan \zeta = \kappa (\lambda - 1)/\xi_0'. \tag{4.3}$$

The Bernoulli equation for flow along a field line gives

$$\tfrac{1}{2}M^2 + \ln p - \tfrac{1}{2}(3x^2 - y^2) = \text{constant}, \tag{4.4}$$

where M is the Mach number with respect to the sound speed s, p is the pressure, and we have expanded the gravitational and centrifugal potential to second-order in x, y. (The potential is independent of the toroidal motion.) The continuity relation implies that

$$p \propto M^{-1} [1 + (dx/dy)^2 \sec^2 \zeta]^{1/2}. \tag{4.5}$$

Combining these two equations, we can deduce that the sonic point ($M = 1$) will be found when

$$y = 3x\,(dx/dy) - \frac{(dx/dy)\,(d^2x/dy^2)}{\cos^2 \zeta + (dx/dy)^2}. \tag{4.6}$$

Now, let the field line be hyperbolic

$$\xi_0'^2 y^2 = x^2 + 2x, \tag{4.7}$$

© Royal Astronomical Society • Provided by the NASA Astrophysics Data System

1982MNRAS.199..883B

with $\xi_0'^2$ chosen to match on to our standard solution. By equating the mass flux through the sonic point to the mass flux in the MHD solution, we find that

$$m = \kappa\,(s/\omega r_0)\,[1 + (dx/dy)^2 \sec^2\zeta]^{-1/2} \tag{4.8}$$

at the sonic point. For our standard solution we find that the sonic point is located at $x = 0.26$, $y = 0.48$, with $m = 0.020\,(s/\omega r_0) \ll 1$. This demonstrates that it is possible for a flow to pass smoothly through a sonic point, and still be regarded as injected from rest and cold as far as the magnetohydrodynamic analysis is concerned. Note that the gas pressure in the vicinity of the sonic point is $O(s/v_{\rm Kep})\,B_0^2/4\pi$, which is of the same order as the potential energy density. This confirms that neither gas pressure gradients nor gravitational forces can influence the field line geometry within the corona above the disc, and that the magnetic field must be essentially force-free. However, within the disc itself, we envisage that the gas pressure greatly increases and that the fluid is gas-dominated.

5 Discussion

In Section 3 we presented the results of a numerical integration of the MHD equations for self-similar, axisymmetric flow from an accretion disc, demonstrating the possiblity of obtaining well-collimated, super-Alfvénic flows. Here we discuss these results in the context of a model of an active galactic nucleus involving a massive black hole surrounded by an accretion disc.

In the vicinity of the disc, the magnetic field will be force-free, with the toroidal and poloidal components having relative strengths

$$\left|\frac{B_\phi}{B_{\rm p}}\right| = \frac{\kappa\,(\lambda - 1)}{(1 + \xi_0'^2)^{1/2}} \quad (\lesssim 1). \tag{5.1a}$$

Very far from the disc the inertia of the matter will have caused the field to become predominantly toroidal. Then

$$\left|\frac{B_\phi}{B_{\rm p}}\right| \simeq \left(\frac{m}{n}\right)^{1/2} \quad (\gg 1). \tag{5.1b}$$

For our standard model (with $\kappa = 0.03$ and $\lambda = 30$), $|B_\phi/B_{\rm p}|_0 \simeq 0.5$, while $|B_\phi/B_{\rm p}|_\infty \simeq 8$.

If the disc deposits mass, energy and angular momentum in the corona, then in a steady state these must be balanced, at the base of the magnetosphere, by the matter flux $j = \kappa\,(B_0^2/4\pi)\,(GM/r_0)^{-1/2}\,(1+\xi_0'^2)^{-1}$, the energy flux $je = \kappa\,(\lambda - 3/2)\,(B_0^2/4\pi)\,(GM/r_0)^{1/2}\,(1+\xi_0'^2)^{-1}$ and the angular momentum flux $jl = \kappa\lambda\,(B_0^2/4\pi) r_0\,(1+\xi_0'^2)^{-1}$. For a given magnetic field structure, κ and λ can be regarded as being fixed by the energy and angular momentum supplied to the corona. This in turn fixes the matter flux j. Note that the maximum energy to angular momentum ratio in the jet is $e/l = \omega$, and this occurs when magnetic stresses predominate ($\lambda \to \infty$). As the energy release is reduced, the Alfvén point (located at the radius $\lambda^{1/2} r_0$) is brought in to smaller radii and the ratio of the magnetic to the particle angular momentum flux $(\lambda - 1)$ (see equation 5.8), is also reduced. The flow is probably self-regulating in the sense that, if an additional torque is applied at the base of the corona, the azimuthal field B_ϕ will be increased and the angular momentum carried away from the disc thereby increased. Similarly, if there is an extra amount of energy deposited, the gas will heat up and its scale height will increase. The mass and energy fluxes will then increase.

© Royal Astronomical Society • Provided by the NASA Astrophysics Data System

1982MNRAS.199..883B

As we remarked in the introduction, the local release of binding energy per unit angular momentum when an element of gas shrinks its orbit is ω, or $e/l=\omega(1-1/\lambda)$. Differential rotation in the disc will, however, lead to a continual shearing of radial field lines which must be balanced, on average, by reconnection processes (e.g. Lynden-Bell 1969; Eardley & Lightman 1975). There will be internal viscous stresses associated with these fields and an associated dissipation which can increase the e/l ratio by a factor of up to 3 (Pringle & Rees 1972). In this case, either the wind will become hot and the thermal terms in equations (2.2) and (2.5) important, or the surplus energy can be radiated away. It is our basic hypothesis that, in some time-averaged sense, most of the angular momentum is carried off locally by the jet, and that whatever energy is not radiated locally must also be transported dynamically.

We can compare the internal torque caused by magnetic stresses acting within the disc with the torque exerted on the surface of the disc by the magnetosphere. Let the mean disc field be $B_d=bB_{0z}$ and estimate the disc thickness as $(2s_d/\omega)$, where s_d is the sound speed in the disc. If the shear stress acting within the disc is written as $\alpha B_d^2/4\pi$, then the ratio of the internal to the surface torque is $(\alpha b^2/2\kappa\lambda)(s_d/\omega r)$. In our solutions, $\kappa\lambda\sim 1$. There is no reliable theory with which to estimate αb^2, but if it does not greatly exceed unity, then in the inner parts of the disc, where $s_d \ll \omega r$, internal stresses should be negligible compared with surface stresses.

In our solutions, the mass loss is constant from each decade of disc radius, producing a total matter flux, from both sides of a disc extending from $r_{0\min}$ to $r_{0\max}$ ($\gg r_{0\min}$), of

$$\dot{M}=\frac{\kappa}{(1+\xi_0'^2)}\,(B_0^2 r_0^2)\left(\frac{GM}{r_0}\right)^{-1/2}\ln(r_{0\max}/r_{0\min}). \tag{5.2}$$

The energy comes mostly from the inner parts of the disc, with a total power at infinity of

$$L=\frac{\kappa}{(1+\xi_0'^2)}\,(\lambda-3/2)\,[B_0^2(r_{0\min})\,r_{0\min}^2]\left(\frac{GM}{r_{0\min}}\right)^{1/2}. \tag{5.3}$$

L may be well in excess of the Eddington limit. In the vicinity of the disc, most of this flux is in magnetic form, the ratio of the Poynting flux to the kinetic energy flux being

$$\frac{F_{\text{Poynting}}}{F_{\text{kinetic}}}=2(\lambda-1). \tag{5.4}$$

In the far-field there are two types of behaviour,

$$\frac{F_{\text{Poynting}}}{F_{\text{kinetic}}}=2, \qquad n\to 1 \text{ asymptotically} \tag{5.5a}$$

$$=\frac{2}{n-2}, \quad n>1 \text{ asymptotically}, \tag{5.5b}$$

with n again being the square of the fast-mode Mach number. Our typical models have $n\gg 1$, and hence correspond to flows in which most of the energy is in the form of bulk kinetic energy of the poloidal flow. This mechanism for magnetically extracting mass and energy from an accretion disc can be very efficient. If a fraction ϵ of the binding energy at $r_{0\min}$ is carried off by a jet, then the ratio of the jet discharge to the disc mass accretion rate $\dot{M}_d$ is

$$\frac{\dot{M}}{\dot{M}_d}=\epsilon\frac{\ln(r_{0\max}/r_{0\min})}{(2\lambda-3)}. \tag{5.6}$$

© Royal Astronomical Society • Provided by the NASA Astrophysics Data System

1982MNRAS.199..883B

Even if $\epsilon \sim 1$, in a magnetically dominated jet ($\lambda \gg 1$) only a small fraction of the accreted gas need participate in the outflow.

The inflow velocity in the disc, v_r, is undetermined in this approach. It may be estimated in terms of β, the ratio of the gas pressure to the magnetic pressure in the disc, as $v_r/s_d = \kappa\lambda/b^2\beta$. In general, we expect that $v_r \ll s_d$.

The angular momentum removed comes mostly from the outer parts of the disc, with a total torque

$$G = \frac{2\kappa\lambda}{(1+\xi_0'^2)} B_0^2(r_{0\max})\, r_{0\max}^3. \tag{5.7}$$

The ratio of the magnetic angular momentum flux to the particle angular momentum flux in the vicinity of the disc is

$$\frac{l_{\text{magnetic}}}{l_{\text{particle}}} = (\lambda - 1). \tag{5.8}$$

In the far-field there are again two types of behaviour.

$$\frac{l_{\text{magnetic}}}{l_{\text{particle}}} = \frac{2\lambda - 3}{\lambda + 3}, \qquad n \to 1 \text{ asymptotically} \tag{5.9a}$$

$$= \frac{2\lambda - 3}{(n-2)\lambda + 3}, \quad n > 1 \text{ asymptotically.} \tag{5.9b}$$

Our typical models, then, have most of the angular momentum flux in the particles in the far-field.

It is also of interest to compute the thrust T of the jet in the far-field,

$$T = \frac{2\kappa(2\lambda/3 - 1)^{1/2}}{(1+\xi_0'^2)} B_0^2(r_{0\min})\, r_{0\min}^2, \quad n \to 1 \text{ asymptotically} \tag{5.10a}$$

$$= \frac{2\kappa(2\lambda - 3)^{1/2}}{(1+\xi_0'^2)} B_0^2(r_{0\min})\, r_{0\min}^2, \quad n > 1 \text{ asymptotically.} \tag{5.10b}$$

With this mechanism of jet production, the jet has a different velocity at each radius. Gas driven from the inner edge of the disc will have a high velocity, while gas driven from the outer parts of the disc will have a much lower velocity. For self-consistency, $r_{0\min}$ cannot be too close to the black hole, or the velocity at infinity on flow lines leaving $r_{0\min}$ will become relativistic. We can compute a characteristic velocity typical of the flow, $\langle v \rangle \equiv T/\dot{M}$. Then,

$$\langle v \rangle = 2(2\lambda/3 - 1)^{1/2} \frac{(GM/r_{0\min})^{1/2}}{\ln(r_{0\max}/r_{0\min})}, \quad n \to 1 \text{ asymptotically} \tag{5.11a}$$

$$= 2(2\lambda - 3)^{1/2} \frac{(GM/r_{0\min})^{1/2}}{\ln(r_{0\max}/r_{0\min})}, \qquad n > 1 \text{ asymptotically.} \tag{5.11b}$$

The magnetic flux emerging from the disc surface can also be computed as $(8\pi/3)$ $B_0(r_{0\max})\, r_{0\max}^2 (1+\xi_0'^2)^{-1/2}$. Note that, as $B_0 \propto r_0^{-5/4}$, most of the magnetic field is contained

© Royal Astronomical Society • Provided by the NASA Astrophysics Data System

1982MNRAS.199..883B

Table 2. Mass flux, power, torque, thrust and characteristic asymptotic velocity for a variety of jet solutions. These results correspond to a jet emerging from an accretion disc extending from $r_{0\min} = 10 r_g$ (with $r_g = GM/c^2$), to $r_{0\max} = 10^3 r_{0\min}$ (where the Keplerian orbital velocity is 3000 km s^{-1}) around a black hole of mass $M = 10^8 M_\odot$. The quoted magnetic field strengths are for $r_{0\min}$.

κ	λ	$\log B_0$ (Gauss)	$\log \dot{M}$ ($M_\odot$ yr^{-1})	$\log L$ (erg s^{-1})	$\log G$ (dyne cm)	$\log T_\infty$ (dyne)	$\langle v_\infty/c \rangle$
0.3	15	2	−4.3	41.7	47.8	31.6	0.5
		4	−0.3	45.7	51.8	35.6	
0.1	10	2	−4.1	41.8	47.9	31.8	0.4
		4	−0.1	45.8	51.9	35.8	
0.03	30	2	−4.7	41.7	47.7	31.5	0.7
		4	−0.7	45.7	51.7	35.5	

in the outer parts of the jet. The total flux threading the disc ($\sim 10^{32}$–10^{36} G cm^2) is relatively small compared with the total flux invoked in non-thermal models of galactic nuclei.

In Table 2 we display values of $\dot{M}, L, G, T_\infty$ and $\langle v_\infty \rangle$ for different jet solutions from a disc around a 10^8-$M_\odot$ black hole in a galactic nucleus. Fields of strength $\sim 10^2$–10^4 G near the black hole are necessary to supply jets with powers in the range $\sim 10^{41}$–10^{46} erg s^{-1} characteristic of extragalactic radio sources. The apparent heterogeneity of observed jets can easily be accommodated within the framework of this model by varying B, M and the size of the disc. In particular, for $\lambda \gg 1$, relativistic jet velocities can be produced by flow from parts of the accretion disc orbiting with speeds $\ll c$.

As we have emphasized, the purpose of the self-similar solution has been to demonstrate explicitly that a magnetically focused jet outflow can indeed be established. Real jets are undoubtedly far more complex (*cf.* Fig. 5). The magnetic field may not have the same polarity everywhere and may instead adopt a sector structure as in the solar wind. Indeed, the most controversial assumption of this whole model is the existence of a dynamically important amount of open magnetic field (*cf.* Parker 1973). Magnetic flux will be continously convected inwards by the accreting gas. Closed magnetic field will be continuously regenerated by dynamo action within the disc (e.g. Pudritz 1981), and explosive reconnection will probably cause a significant power to be dissipated via magnetic flares within the disc corona (e.g. Galeev, Rosner & Vaiana 1979). The outflow associated with flares can then convect magnetic flux outwards. If the field lines are carried well beyond the Alfvén and magnetosonic points before they reconnect, then this field too can be regarded as effectively open.

The far field is also not immune from instability. There is a strong velocity shear within our solutions and, when the energy flux is carried mainly by the particles, as it is beyond the critical points, we expect the flow to become locally unstable. The non-linear development of these instabilities will lead to the transport of linear and angular momentum throughout the jet. In particular, the toroidal component of magnetic field will probably try to minimize its energy by scaling inversely with cylindrical radius.

In constructing self-similar solutions, we have implicitly ignored the boundary conditions at large and small radii. We are assuming that the magnetic and inertial stresses associated with the flow emerging from $r_0 \sim r_{0\max}$ can be balanced by external pressure associated with the surrounding medium. In practice, the jet will probably expand or contract to achieve this pressure balance. The surface of the jet may also be subject to Kelvin–Helmholtz type instabilities (e.g. Ferrari, Trussoni & Zaninetti 1977; Payne & Cohn 1982, in preparation;

© Royal Astronomical Society • Provided by the NASA Astrophysics Data System

1982MNRAS.199..883B

Cohn 1982), whose non-linear development will cause entrainment of surrounding gas and deceleration of the jet. Most of the power carried by the jet flows up the central core. We have terminated our solutions at $r_{0\min} \sim 10r_g$, because our assumptions of self-similarity and subrelativistic speeds begin to break down. Magnetic torques can, however, be just as effective in removing orbital energy and angular momentum from the innermost parts of the disc, and also from a spinning black hole (Blandford & Znajek 1977; MacDonald & Thorne 1982). The existence of a magnetic torque acting on the disc requires that a radial current flow in the disc. The circuit must be completed by currents flowing in the core ($r \lesssim r_{0\min}$) and within or beyond the wall ($r \gtrsim r_{0\max}$).

We have also ignored the effects of thermal pressure, except within the disc corona. Many galactic nuclei, including most radio quasars, are powerful X-ray sources, and so the outflowing gas can be Compton heated to temperatures $\sim 10^7$–10^8 K. In the limit of low magnetic field, a thermally driven outflow can be established in the outer regions of the disc (Begelman, McKee & Shields 1982, in preparation), although, in this case, we do not expect the flow to be collimated directly. Instabilities in the super-Alfvénic portion of the flow can also cause dissipation and thus, as we have argued in Section 3, heat the gas enough to prevent the jet from pinching off.

Finally, we emphasize that this mechanism is not specific to an accretion disc surrounding a massive black hole. It can also operate in stellar mass objects, including those with central neutron stars. It may be responsible for generating the double source associated with Sco X-1 and may even cause the precessing jets in SS 433.

Acknowledgments

We thank J. Bardeen for sending us a helpful description of unpublished calculations of hydrodynamical flows above accretion discs, R. Flammang for several useful discussions on critical point theory and D. MacDonald for assistance with some of the numerical work. We also thank the Director of the Institute of Astronomy, Cambridge, for hospitality during the summers of 1979 and 1981.

This work was supported in part by NSF grant AST 80-17752. R.D.B. is an Alfred P. Sloan Foundation Research Fellow.

References

Bardeen, J. M. & Berger, B., 1978. *Astrophys. J.*, **221**, 105.
Bardeen, J. M. & Petterson, J. A., 1975. *Astrophys. J.*, **195**, L65.
Bicknell, G. V. & Henriksen, R. N., 1980. *Astrophys. Lett.*, **21**, 29.
Blandford, R. D., 1976. *Mon. Not. R. astr. Soc.*, **176**, 465.
Blandford, R. D. & Znajek, R. L., 1977. *Mon. Not. R. astr. Soc.*, **179**, 433.
Braes, L. L. E. & Miley, G. K., 1971. *Astr. Astrophys.*, **14**, 160.
Butcher, H. R., van Breugel, W. & Miley, G. K., 1980. *Astrophys. J.*, **235**, 749.
Chan, K. L. & Henriksen, R. N., 1980. *Astrophys. J.*, **241**, 534.
Chandrasekhar, S., 1956. *Astrophys. J.*, **124**, 232.
Cohn, H., 1981. Preprint.
Curtis, H., 1918. *Pub. Lick Obs.*, **13**, 31.
Eardley, D. M. & Lightman, A. P., 1975. *Astrophys. J.*, **200**, 187.
Feigelson, R. *et al.*, 1981. *Astrophys. J.*, **251**, 31.
Ferrari, A., Trussoni, E. & Zaninetti, L., 1978. *Mon. Not. R. astr. Soc.*, **182**, 49.
Ferraro, V. C. A., 1937. *Mon. Not. R. astr. Soc.*, **79**, 458.
Galeev, A. A., Rosner, R. & Vaiana, G. S., 1979. *Astrophys. J.*, **229**, 318.
Henriksen, R. N. & Rayburn, D. R., 1971. *Mon. Not. R. astr. Soc.*, **152**, 323.
Hjellming, R. M. & Johnson, K. J., 1981. *Nature*, **290**, 100.
Jones, T. W. & O'Dell, S. L., 1977. *Astr. Astrophys.*, **61**, 291.

© Royal Astronomical Society • Provided by the NASA Astrophysics Data System

1982MNRAS.199..883B

Lovelace, R. V. E., 1976. *Nature,* **262,** 649.
Lynden-Bell, D., 1969. *Nature,* **223,** 690.
MacDonald, D. & Thorne, K. S., 1982. *Mon. Not. R. astr. Soc.,* **198,** 345.
Margon, B., 1982. *Proc. Tenth Texas Symp. on Relativistic Astrophysics,* in press.
Mestel, L., 1961. *Mon. Not. R. astr. Soc.,* **122,** 473.
Miley, G. K., 1980. *A. Rev. Astr. Astrophys.,* **18,** 165.
Mouschovias, T. & Paleologou, E. V., 1980. *Moon Planets,* **22,** 31.
Ozernoi, L. M. & Usov, V. V., 1973. *Astrophys. Space Sci.,* **25,** 149.
Parker, E. N., 1973. *Astrophys. Space Sci.,* **24,** 279.
Perley, R. A., Willis, A. G. & Scott, J. S., 1979. *Nature,* **281,** 437.
Piddington, J. H., 1970. *Mon. Not. R. astr. Soc.,* **148,** 131.
Pringle, J. E. & Rees, M. J., 1972. *Astr. Astrophys.,* **21,** 1.
Pudritz, R. & Fahlman, G. G., 1982. *Mon. Not. R. astr. Soc.,* **198,** 689.
Readhead, A. C. S., Cohen, M. H., Pearson, T. J. & Wilkinson, P. N., 1978. *Nature,* **276,** 768.
Rees, M. J., 1978. *Nature,* **275,** 516.
Schmidt, M., 1963. *Nature,* **197,** 1040.
Shakura, N. I. & Sunyaev, R. A., 1973. *Astr. Astrophys.,* **24,** 337.
Sturrock, P. A. & Barnes, C., 1972. *Astrophys. J.,* **176,** 31.
Wardle, J. F. C., 1977. *Nature,* **269,** 563.
Weber, E. J. & Davis, L., 1967. *Astrophys. J.,* **148,** 217.
Withbroe, G. L. & Noyes, R. W., 1977. *A. Rev. Astr. Astrophys.,* **15,** 363.
Zel'dovich, Ya. B. & Novikov, I. D., 1971. *Relativistic Astrophysics,* vol. 1: *Stars and Relativity,* University of Chicago Press, Chicago.

© Royal Astronomical Society • Provided by the NASA Astrophysics Data System